PCIM Europe 2018; International Exhibition and Conference for Power Electronics, Intelligent Motion, Renewable Energy and Energy Management; Proceedings of

MMC-based High Power DC-DC Converter Employing Scott Transformer

S. Milovanovic and D. Dujic

POWER ELECTRONICS LABORATORY
ÉCOLE POLYTECHNIQUE FÉDÉRALE DE LAUSANNE

MMC-based High Power DC-DC Converter Employing Scott Transformer

Stefan Milovanović, Dražen Dujić
Power Electronics Laboratory, École Polytechnique Fédérale de Lausanne (EPFL), Switzerland
stefan.milovanovic@epfl.ch, drazen.dujic@epfl.ch

Abstract

HVDC transmission, along with MVDC distribution grids, have been gaining more and more attention lately. With the aim of obtaining resilient and flexible DC grid, reliable means for interfacing two of its parts operating under different voltage levels must be ensured. This paper proposes bidirectional, isolated, high step-down, MMC-based, DC-DC converter intended to connect high/medium voltage bipolar DC grid and low voltage DC grid. In order to achieve galvanic separation between two converter stages, Scott transformer connection was used.

1. Introduction

Continuously growing electrical energy consumption demands, have resulted in the need for the existing power system transmission capacity increase. Therefore, the ideas of converting an AC power line into DC have emerged during 1970s [1]. Consequently, transmission capacity of a line can be increased by the factor of almost 3, while using the same Rights of Way (ROW). Depending on the type of an AC line, different DC circuit configurations are possible [2]–[4]. Although the least promising in terms of transmission capacity increase, bipolar DC networks with return (neutral) conductor brought system redundancy concept into the spotlight. Namely, if either of DC poles happens to be lost, system can continue to operate utilizing the neutral conductor, although with reduced power. Hence, system reliability improvement is achieved. Nevertheless, regardless of a DC system nature, DC-DC converter can be considered its key part providing the means for connecting parts operating under different voltages and controlling the energy flow between them. Further, DC systems offer another convenient property. Unlike their AC counterparts, isolation stages usually present within DC-DC converters can be designed to operate at any arbitrary frequency. Therefore, bulky Low Frequency Transformer (LFT) can be replaced by more compact Medium Frequency Transformer (MFT). However, accepting High Voltage (HV)/Medium Voltage (MV) at either of a DC-DC converter stages can be quite challenging if series connection of power switches were to be engaged. With the aim of facilitating HV/MV handling, Modular Multilevel Converter (MMC) consisting of series connection of so-called submodules (SMs) can be employed. MMC-based topologies have been subject to various research projects [5]–[8]. In [5], MMC-based Single-Phase (1PH) Dual-Active Bridge (DAB) was thoroughly analyzed, whereas new control method implying sequential insertion of MMC-alike SMs was proposed in [6], [7]. However, employment of MMC-based DAB topologies has not been analyzed within bipolar grids with neutral conductor.

In [9] topology employing Three-Phase (3PH) Three-Winding Transformer, with the aim of exploiting the aforementioned redundancy principle, is proposed. However, two 3PH MMCs in the HV/MV stage are not irreplaceable in the process of obtaining symmetrical system of 3PH Low Voltage (LV) stage currents. Scott Transformer Connection (STC), which has mostly been used within the railway applications so far, can as well be used to obtain symmetrical system of 3PH currents out of two 1PH voltage sources. Unlike the topology presented in [9], two 1PH transformers can be employed, thus reducing overall complexity of the system. This paper proposes bidirectional, isolated, high step-down DC-DC converter utilizing STC, operating in the medium frequency range, to achieve galvanic isolation along with voltage matching.

ISBN 978-3-8007-4646-0

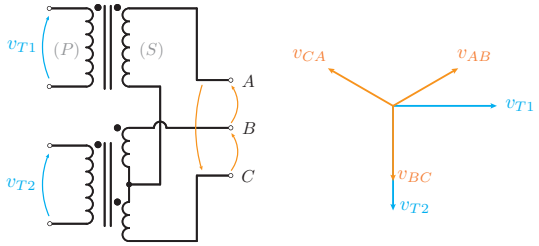

Fig. 1: STC with its voltage phasor diagram.

2. Topology operating principles

Fig. 1 presents STC with its voltage phasor diagram. T_2 Secondary (S) winding is divided into two parts, both having number of turns equal to $N/2$. In order to ensure proper STC operation, T_1 S-winding number of turns has to be set as $N\sqrt{3}/2$. Consequently, providing both transformers Primary (P)-winding number of turns equality, turns ratios relation can be derived as $m_{T1} = 2m_{T2}/\sqrt{3}$. To the best knowledge of the authors, no publications have ever analyzed the employment of STC, operating in the medium frequency range, within the field of high power DC-DC conversion.

Fig. 2 presents proposed converter consisting of two series connected MMCs in the HV/MV stage and Six-Step Converter (SSC) in the LV stage. In order to interface HV/MV grid, both MMCs use Half-Bridge (HB) SMs. Number of HB SMs depends upon available HV/MV and voltage class of semiconductors employed within the MMCs. SSC operates with square-wave voltages (at MFT operating frequency) with the aim of minimizing switching losses. It can be shown that voltages across T_1 and T_2 P-windings (v_{T1} and v_{T2}, respectively) correspond to the combination of LV side quantities, according to (1)-(2).

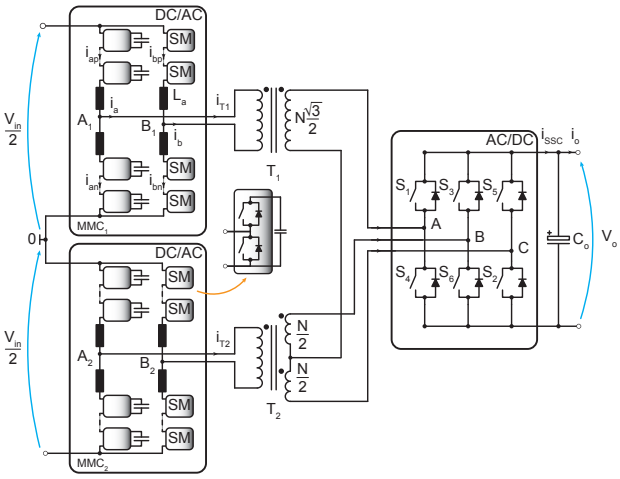

Fig. 2: Proposed topology consisting of two series connected MMCs in the HV/MV stage (since bipolar grid with neutral conductor is available), STC and conventional SSC in the LV stage.

$$v_{T1} = m_{T1}\frac{v_{AB} - v_{CA}}{2} \tag{1}$$

$$v_{T2} = m_{T2}v_{BC} \tag{2}$$

It can be seen from Fig. 3 that voltages v_{T1} and v_{T2} differ. However, MMC provides the possibility of arbitrary voltage waveform generation, as long as energy balances within the converter are maintained. Fig. 3a depicts equivalent circuits of both MMCs connected to their associated transformers. If appropriate voltage waveforms were to be generated by the MMCs, energy transfer could be controlled by adjusting the phase shift φ between the observed MMC AC voltage and its transformer EMF.

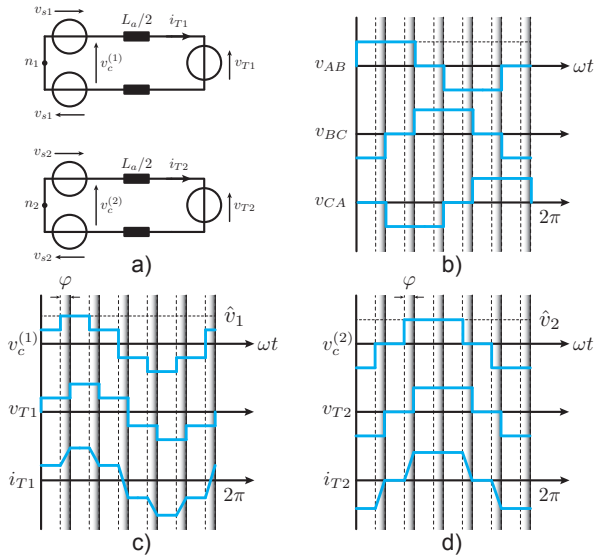

Fig. 3: a) Equivalent circuits of two MMCs connected to T_1 and T_2, respectively b) Line voltages created by the SSC at converter's LV side c) Waveforms relevant for T_1 power flow analysis d) Waveforms relevant for T_2 power flow analysis.

ISBN 978-3-8007-4646-0

Figs. 3c and 3d present appropriate voltage waveforms to be generated by the MMCs, as well as currents flowing through both transformers P-windings. Based on transformers turns ratios relation, expressions (1)-(2) and Fig. 3b, peak voltages $\hat{v}_1$ and $\hat{v}_2$ can be calculated. If output voltage reference value was denoted by V_o, then $\hat{v}_1 = m_{T1}V_o$ and $\hat{v}_2 = m_{T2}V_o$. By analyzing the waveforms given by Fig. 3c and 3d, power at which the energy is flowing through T_1 and T_2 can be derived (3)-(4).

$$P_{T1} = \frac{\hat{v}_1^2}{\omega L_\Sigma}\varphi_1\left(\frac{1}{2} - \frac{3\varphi_1}{8\pi}\right) = \frac{m_{T1}^2 V_o^2}{\omega L_\Sigma}\varphi_1\left(\frac{1}{2} - \frac{3\varphi_1}{8\pi}\right) \quad (3)$$

$$P_{T2} = \frac{\hat{v}_2^2}{\omega L_\Sigma}\varphi_2\left(\frac{2}{3} - \frac{\varphi_2}{2\pi}\right) = \frac{m_{T2}^2 V_o^2}{\omega L_\Sigma}\varphi_2\left(\frac{2}{3} - \frac{\varphi_2}{2\pi}\right) \quad (4)$$

If either of the MMCs from Fig. 2 were to be observed, according to Fig. 3a, one might conclude that adjacent branches of either MMC have to generate two voltages of the same amplitude, however with phases opposite with respect to each other. This means that the observed MMC branches can be controlled in complementary manner. In other words, a branch AC pole reference voltage v_{si} will be used with the opposite sign for the adjacent one. In (3) and (4) L_Σ accounts for the sum of a MMC arm inductance and its associated transformer leakage inductance.

3. System Design

3.1. Transformers turns ratios

In order to effectively control converter power flow, amplitudes of both MMCs AC voltages need to match the ones of their associated transformers EMFs, while simultaneously preserving SMs energy balance. T_1 voltage amplitude proves to be higher compared to T_2, therefore MMC_1 needs to create higher voltage across its AC terminals. Hence, it will be considered critical in terms of transformer turns ratio determination. However, certain number of SMs within an arm needs to be disposable for the purpose of energy balance preservation (in this paper, such design and control approach is considered). Consequently, AC voltage generated across MMC_1 AC terminals gets reduced by a certain factor $\zeta < 1$ (5).

$$\hat{v}_1 = \zeta\frac{Vin}{2} \quad (5)$$

Considering that (5) must be equal to the amplitude of voltage across T_1 P-winding, (6) can easily be derived. Bearing the relationship between T_1 and T_2 turns ratios in mind, (7) follows.

$$m_{T1} = \zeta\frac{V_{in}}{2V_o} \quad (6)$$

$$m_{T2} = \zeta\sqrt{3}\frac{V_{in}}{4V_o} \quad (7)$$

By substituting (6)-(7) into (3)-(4), one might realize that $P_{T1} = P_{T2}$ providing $\varphi_1 = \varphi_2$. On these terms, another convenient property of the proposed topology becomes obvious - LV side 3PH currents correspond to 3PH DAB currents [10], as will be seen in section 5. Furthermore, only one phase angle can be used within the control system considering that transformers share the total system power equally.

3.2. MMC arm inductor design

Considering inevitable presence of arm inductors within both MMCs, double role can be assigned to them. On one hand, arm inductors are used to limit MMC common-mode current ripple originating from voltage oscillations across MMC SMs. On the other hand, MMC arm inductors can be used to control the converter power transfer since a MMC equivalent inductance seen from its associated transformer P-winding equals its arm inductance. Of course, this statements holds providing transformers' leakage inductances can be considered negligible compared to MMC arm inductances. Therefore, for a given system rated power P_{nom}, operating frequency f and nominal phase angle φ_{nom}, arm inductance can be calculated according to (3) or (4).

3.3. SMs capacitor design

Both MMCs were controlled in a conventional closed-loop manner. Harmonic components of all the currents flowing through an arm were calculated. Thereafter, arm energy variation was calculated utilizing information on several most dominant harmonics and SM capacitance was determined as proposed in [11].

3.4. Output capacitor design

Output capacitor can be designed by several different criteria. However, the one being employed within the above analysis reflects to the abrupt load changes in the LV stage. Capacitance providing desired voltage drop (ΔV_o) over a predefined period (T_D), during which any converter actions upon abrupt load connection are either forbidden or not triggered by the control system, can be selected as (8), where R_o denotes the resistance of maximum permissible load to be abruptly connected.

$$C_o \geq -\frac{T_D}{R_o ln\left(1-\frac{\Delta V_o}{V_o^*}\right)} \tag{8}$$

4. System control

Analyzed system parameters can be seen in Table 1. Output voltage control was performed according to Fig. 4, with the aim of maintaining the output voltage mean value equal to the reference given by the table below. Seen from the load side, SSC can be perceived as an ideal current source owing to the fact that DAB-based circuit output current does not depend on its output voltage. Therefore, one might conclude that in order to regulate the output voltage, SSC output current mean value $\overline{i_R}$ should be adjusted. However, variable to be affected within DAB-alike systems is the phase shift between relevant voltage waveforms. Therefore,

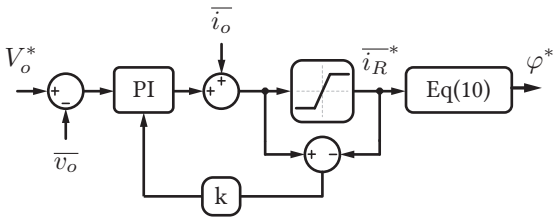

Fig. 4: Output voltage control implementation.

phase angle φ information needs to be extracted from the SSC output current reference. Observing (3) and (4), one might connect SSC output current average value with HV/MV quantities, however this would result in the need for solving non-linear equations.

Linearization of power curves given by (3) and (4) around desired operating angle can be performed. It can be shown that this will not significantly hinder the precision of obtained results. Ultimately, voltage regulator will compensate for the errors introduced by the aforementioned linearization. If linearization point were chosen as $\varphi = \pi/6$, system power curve can be rewritten as (9).

$$P_o = \frac{7\zeta V_{in} v_o m_{T1}}{16\omega L_\Sigma}\varphi \tag{9}$$

Given that output power can be perceived as the product of SSC output current mean value and output voltage, phase angle information can be extracted from SSC output current reference based on (10).

$$\varphi = \frac{16\omega L_\Sigma}{7\zeta V_{in} m_{T1}}\overline{i_R}^* \tag{10}$$

Moreover, owing to the fact that whole converter can be modeled with an ideal current source seen from the load side, load current can be used as a feed-forward variable.

Table 1: Analyzed system parameters

Input voltage (V_{in})	Output voltage (V_o)	Rated power (P_{nom})	System operating frequency (f)
40kV	1.5kV	10MW	1kHz

ISBN 978-3-8007-4646-0

Table 2: Passive components design

MMC arm inductance (L_a)	1 mH
SMs capacitance (C_{SM})	5mF
Output filter capacitance (C_o)	10mF
Number of SMs per arm (N)	20

5. Simulation results

Proposed high-power DC-DC converter was modeled and simulated in PLECS. Table 2 presents values of passive components used within the simulation. Number of SMs needs to be chosen according to the voltage class of available semiconductor devices. However, for the sake of presenting converter performance it was set as $N = 20$. Fig. 5 presents converter operating waveforms.

Load was modeled as parallel connection of two resistors whose equivalent resistance corresponds to the consumption of the system rated power under the rated output voltage. Firstly, at time instant denoted by $t = t_1$, half the rated load was connected to the LV bus. Certain output voltage V_o drop can be observed, along with an overshoot originating from the structure of the controller being employed. Thereafter, at time instant denoted by $t = t_2$, the other half of the load was connected to the LV bus. It can be seen that, once again, output voltage drops however it recovers within a few converter operating periods. It is noteworthy that, even though output voltage exhibits abrupt changes due to the load connection/disconnection, abrupt phase angle changes must not be allowed within the 3PH DAB as it would cause LV stage currents unbalance [12], [13].

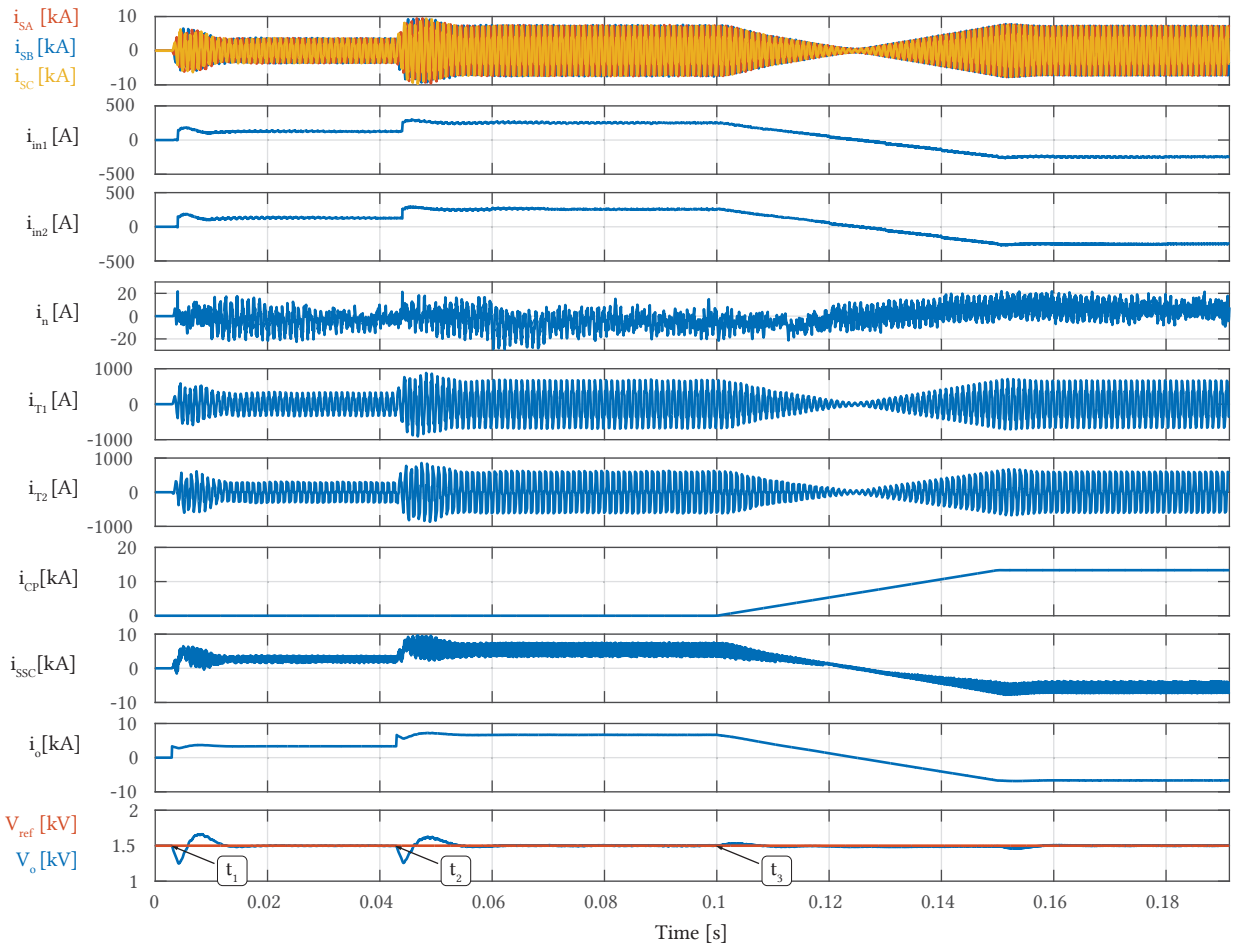

Fig. 5: Converter operating waveforms.

ISBN 978-3-8007-4646-0

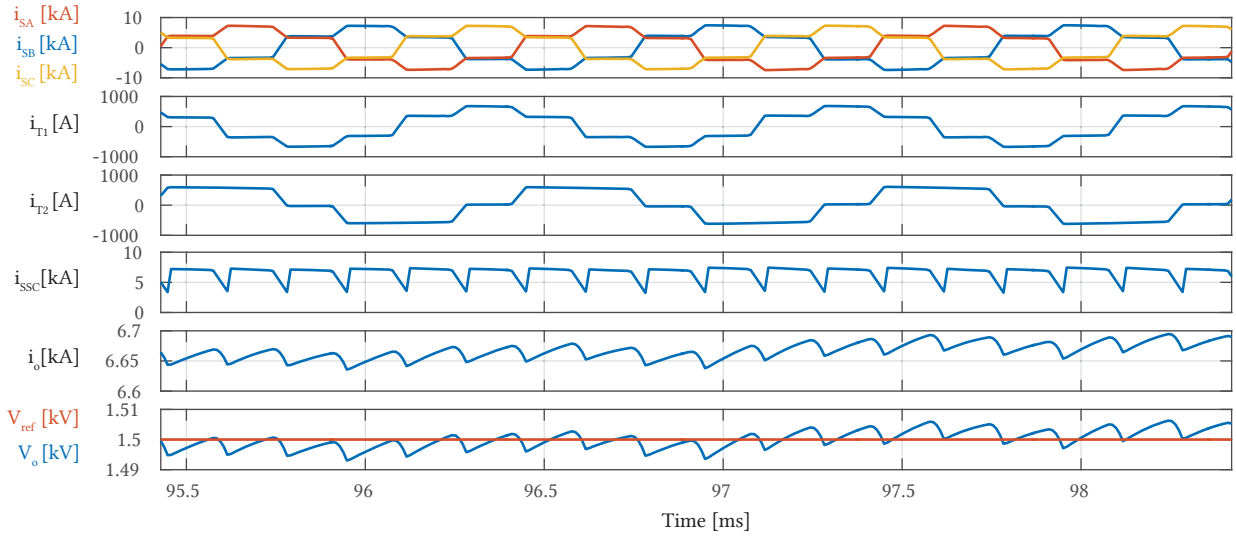

Fig. 6: Converter operating waveforms during three fundamental periods between time instants t_2 and t_3.

It can be shown that the proposed converter behavior can be observed through an equivalent 3PH DAB, however such an analysis falls out of this paper's scope. Therefore, abrupt phase angle changes generated by the control system were treated as proposed in [12], [13].

At time instant $t = t_3$ ideal current source i_{CP} ramping its current up from zero to twice the load nominal current over the period of 50ms gets connected to the LV bus. With the aim of maintaining the output voltage at reference given by Table 1, converter gradually reversed its power during the ideal current source ramp-up time, as can be seen from Fig. 5. Additionally, it can be seen that very small current i_n flows through the return conductor. It equals the difference between MMCs' input currents, which originates from the mismatch in MMCs' balancing current components.

Fig. 6 presents converter operation during three fundamental periods. It can be seen that LV stage 3PH currents (i_{SA}, i_{SB}, i_{SC}) correspond to the ones observed within conventional 3PH DAB. Both T_1 and T_2 P-winding currents correspond to the idealized waveforms presented in Fig. 3. As expected, SSC output current consists of the mean value along with ripple occurring at six times converter operating frequency superimposed. Output voltage consists of the mean value along with ripple originating from the SSC current oscillations. However, ripple occurring at frequency lower than six times converter operating frequency can as well be observed. This is due to the resistances present within both transformers, and if SSC output current were to be zoomed further, these oscillations would be observed as well. However, these oscillations are negligible in magnitude, therefore not affecting the system operation.

6. Conclusion

This paper proposed MMC-based high power DC-DC converter which utilizes STC as means of isolation between HV/MV and LV stages. Instead of employing well known 3PH three-winding transformer, and therefore provide the possibility of exploiting redundancy principle offered by the presence of neutral conductor, two 1PH transformers can be used providing proper form AC voltages are generated by the MMCs. Consequently, system complexity reduction is achieved, while maintaining redundancy principle. If any of the voltage poles happens to be lost, converter would continue to operate in the de-rated mode, however as the 1PH DAB, meaning that slight, not too complicated though, circuit configuration changes have to be performed. Seen from the LV stage, this topology behaves as same as conventional 3PH DAB. Therefore, all LV stage soft-switching properties can be retained.

ISBN 978-3-8007-4646-0

Acknowledgment

This work is in part supported by the Swiss Competence Centers for Energy Research (SCCER) initiative which is supported by the Swiss Commission for Technology and Innovation (CTI) with focus on Future Swiss Electrical Infrastructure (FURIES), and in part by Hyundai Electric Co., LTD., Republic of Korea.

References

[1] A. Clerici, L. Paris, and P. Danfors, "HVDC conversion of HVAC lines to provide substantial power upgrading," *IEEE transactions on Power Delivery*, vol. 6, no. 1, pp. 324–333, 1991.

[2] M. Häusler, G. Schlayer, and G. Fitterer, "Converting AC power lines to DC for higher transmission ratings," *ABB review*, pp. 4–11, 1997.

[3] D. M. Larruskain, I. Zamora, O. Abarrategui, and Z. Aginako, "Conversion of AC distribution lines into DC lines to upgrade transmission capacity," *Electric Power Systems Research*, vol. 81, no. 7, pp. 1341–1348, 2011.

[4] D. M. Larruskain, I. Zamora, O. Abarrategui, and A. Iturregi, "VSC-HVDC configurations for converting AC distribution lines into DC lines," *International Journal of Electrical Power & Energy Systems*, vol. 54, pp. 589–597, 2014.

[5] S. Kenzelmann, A. Rufer, D. Dujic, F. Canales, and Y. R. De Novaes, "Isolated DC/DC structure based on modular multilevel converter," *IEEE Transactions on Power Electronics*, vol. 30, no. 1, pp. 89–98, 2015.

[6] I. Gowaid, G. P. Adam, S. Ahmed, D. Holliday, and B. W. Williams, "Analysis and design of a modular multilevel converter with trapezoidal modulation for medium and high voltage DC-DC transformers," *IEEE Transactions on Power Electronics*, vol. 30, no. 10, pp. 5439–5457, 2015.

[7] I. Gowaid, G. Adam, A. M. Massoud, S. Ahmed, D. Holliday, and B. Williams, "Quasi two-level operation of modular multilevel converter for use in a high-power DC transformer with DC fault isolation capability," *IEEE Transactions on Power Electronics*, vol. 30, no. 1, pp. 108–123, 2015.

[8] S. Cui, N. Soltau, and R. W. De Doncker, "A high step-up ratio soft-switching DC–DC converter for interconnection of MVDC and HVDC grids," *IEEE Transactions on Power Electronics*, vol. 33, no. 4, pp. 2986–3001, 2018.

[9] S. Milovanovic and D. Dujic, "Six-step MMC-based high power DC-DC converter," in *2018 International Power Electronics Conference - Niigata (IPEC-Niigata 2018)*, IEEE, 2018.

[10] R. W. De Doncker, D. M. Divan, and M. H. Kheraluwala, "A three-phase soft-switched high-power-density DC/DC converter for high-power applications," *IEEE transactions on industry applications*, vol. 27, no. 1, pp. 63–73, 1991.

[11] M. Vasiladiotis, N. Cherix, and A. Rufer, "Accurate capacitor voltage ripple estimation and current control considerations for grid-connected modular multilevel converters," *IEEE Transactions on Power Electronics*, vol. 29, no. 9, pp. 4568–4579, 2014.

[12] S. P. Engel, N. Soltau, and R. W. De Doncker, "Instantaneous current control for the three-phase dual-active bridge DC-DC converter," in *Energy Conversion Congress and Exposition (ECCE)*, IEEE, 2012, pp. 3964–3969.

[13] S. P. Engel, N. Soltau, H. Stagge, and R. W. De Doncker, "Dynamic and balanced control of three-phase high-power dual-active bridge DC–DC converters in dc-grid applications," *IEEE Transactions on Power Electronics*, vol. 28, no. 4, pp. 1880–1889, 2013.